Water-Plasma Medium for a Hydrogen Laser

Randell L. Mills, * **Paresh, C. Ray, Robert M. Mayo**

BlackLight Power, Inc., 493 Old Trenton Road, Cranbury, New Jersey 08512

A stationary, electronically-excited, population inversion of atomic hydrogen, H, has been observed in a low pressure water-vapor microwave discharge plasma. The inverted H population was evident from the relative intensities of the transitions within the Lyman series (n = 2, 3, 4, and 5 to n = 1) and within the Balmer series (n = 3, 4, 5, 6, 7, and 8 to n = 2). Lines of the Balmer series of n = 5, and 6 to n = 2 and the Paschen series of n = 5 to n = 3 were of particular importance because of the potential to design blue and 1.3 micron infrared lasers, respectively, which are ideal for many communications and microelectronics applications. High power hydrogen gas lasers are anticipated at wavelengths, over a broad spectral range from far infrared to violet which may be miniaturized to micron dimensions. Such a hydrogen laser represents the first new atomic gas laser in over a decade, and it may prove to be the most versatile and useful of all.

* To whom correspondence should be addressed. Phone: 609-490-1090; Fax: 609-490-1066; E-mail: rmills@blacklightpower.com

I. Introduction

For the last fifteen years there has been an aggressive search for a blue laser. A blue laser would significantly improve the performance of many applications and open new venues. Blue lasers that are durable and bright have significant applications such as superior displays, optical sensors, laser printers and scanners, fiber optical and undersea optical communications, satellite and undersea detection and targeting of submarines, undersea mine detection, undersea salvage, medical devices, and higher density compact disk (CD) players. The shorter (blue) wavelength could be more sharply focused such that the capacity of magnetic and optical storage may be increased. Digital versatile disks (DVDs) which rely on red aluminum indium gallium phosphide (AlInGaP) semiconductor lasers have a data capacity of about 4.7 gigabytes (Gbytes) compared to 0.65 for compact discs. The capacity could be increased to 15 Gbytes with a suitable violet laser. Despite the tremendous value of a blue laser, advancements have been limited due to a lack of materials which emit blue light or blue-emitting plasmas capable of lasing.

Recombination of injected electrons and holes in InGaN has been extensively pursued as a suitable blue laser.[1] Unfortunately, after over a decade of effort with an estimated expenditure of $1 B, blue diode lasers are still plagued by inadequate substrates, crystal layer dislocations, and defects that increase over time with the requisite high drive currents. Frustration over these and other impediments to commercialization of this important device has given rise to the view that commercial success may depend on the discovery of something completely new.[2]

Inverted Lyman and Balmer populations may permit a continuous wave (cw) laser at blue wavelengths. For the last four decades, scientists from academia and industry have been searching for lasers using hydrogen plasma.[3-6] Developed sources that provide a usefully

intense hydrogen plasma are high powered lasers, arcs and high voltage DC and RF discharges, synchrotron devices, inductively coupled plasma generators, and magnetically confined plasmas. However, the generation of population inversion is very difficult. Recombining expanding plasma jets formed by methods such as arcs or pulsed discharges is considered one of the most promising methods of realizing an H I laser.

Because the population of hydrogen states is overwhelmingly dominated by the ground state even in the most intense plasmas, the realization of an H I laser requires an overpopulation in a state with $n_i > 2$ which decays to a state with $1 < n < n_i$. Thus, an H I laser based on a Balmer transition is feasible for a mechanism which produces an overpopulation in a corresponding state. The Balmer α, β, γ, and δ lines of atomic hydrogen at 6562.8 Å, 4861.3 Å, 4340.5 Å, 4101.7 Å in the visible region are due to the transitions from $n = 3$, $n = 4$, $n = 5$, and $n = 6$ to $n = 2$, respectively. An H overpopulation of $n > 3$ that is above threshold could be the basis of a blue laser. But, lasing of a blue Balmer line has been difficult to achieve even with cold recombining plasmas. Akatsuka and Suzuki,[6] for example, were able to achieve an overpopulation for level pairs 4-3 and 5-4 only for a recombining plasma generated in a arc-heated magnetically trapped expanding plasma jet.[6]

Rather than using recombining arcs or recombining electron-hole pairs in semiconductors to achieve lasing at blue wavelengths, a chemical approach was pursued. It was previously reported that a new chemically generated plasma source has been developed that operates by incandescently heating a hydrogen dissociator and a catalyst to provide atomic hydrogen and gaseous catalyst, respectively, which react to produce an energetic plasma called a resonance transfer (rt)-plasma.[7,8] Intense VUV emission was observed at low temperatures (e.g. $\approx 10^3\ K$) and an extraordinary low field strength of about 1-2 V/cm from atomic hydrogen and certain atomized elements or certain gaseous ions which singly or multiply ionize at integer

3

multiples of the potential energy of atomic hydrogen, $E_h = 27.2 \ eV$ where E_h is one hartree. The theory has been given previously.[9,10]

For oxygen, there are several chemical reactions that fulfill the catalyst criterion—a chemical or physical process with an enthalpy change equal to an integer multiple of E_h. The reactions $O_2 \rightarrow O + O^{2+}$, $O_2 \rightarrow O + O^{3+}$, and $2O \rightarrow 2O^+$ provide a net enthalpy of about 2, 4, and 2 times E_h, respectively.[11] Lasing directly from oxygen is unknown, but lasing from inverted water vibration-rotational levels in water plasmas which may be from hydrogen-oxygen mixtures has been achieved several decades earlier.[12] In addition, helium-water plasmas as well as water plasma lasers were explored for a source of submillimeter wavelengths.[13] More recently, emission from $OH^\bullet$ radicals in water and helium-hydrogen water plasmas has been investigated as an efficient source of radiation in the region $\lambda < 2000$ Å for the replacement of expensive working media based on krypton and xenon in microelectronics, photochemistry, and medical applications.[14] These prior water-plasma light sources were based on high-voltage glow discharges. In our experiments, a microwave water plasma was used as a source of O_2 and atomic hydrogen.

II. Experimental

The VUV spectrum (900 – 1300 Å), the width of the 6562.8 Å Balmer α line, and the high resolution visible spectra (4000-7000 Å) were recorded on light emitted from microwave, capacitively coupled RF, inductively coupled RF, and glow discharge water plasmas performed according to methods and setups reported previously.[8–10,15–17] Hydrogen and hydrogen (10%) mixed with xenon, krypton, or nitrogen control plasmas were run under matching conditions. The microwave experimental set up comprised a quartz tube cell, a source of water vapor or

ultrapure control gases, a flow system, and a visible spectrometer or a VUV spectrometer that was differentially pumped. Water vapor was formed in a heated insulated reservoir and flowed through the half inch diameter quartz tube at a flow rate of 10 standard $cm^3 \cdot s^{-1}$ (sccm) at a corresponding pressure of 50-100 milliTorr. At this pressure, room temperature was sufficient for maintaining the water vapor. The tube was fitted with an Evenson coaxial microwave cavity (Opthos) having an E-mode.[18,19] The input power to the plasma at 2.45 GHz by an Opthos model MPG-4M generator was set at 50 W and 90 W as described previously.[9,10,15-17]

The plasma emission was fiber-optically coupled through a 220F matching fiber adapter positioned 2 cm from the cell wall to a high resolution visible spectrometer with a resolution of ±0.06 Å over the spectral range 1900-8600 Å. The spectrometer was a Jobin Yvon Horiba 1250 M with 2400 groves/mm ion-etched holographic diffraction grating. The entrance and exit slits were set to 20 μm. The spectrometer was scanned between 6555-6570 Å and 4000-7000 Å using a 0.05 Å step size. The signal was recorded by a PMT with a stand alone high voltage power supply (950 V) and an acquisition controller. The data was obtained in a single accumulation with a 1 second integration time.

To measure the absolute intensity, the high resolution visible spectrometer and detection system were calibrated[20] with 5460.8 Å, 5799.6 Å, and 6965.4 Å light from a Hg-Ar lamp (Ocean Optics, model HG-1) that was calibrated with a NIST certified silicon photodiode. The population density of the $n = 3$ hydrogen excited state N_3 was determined from the absolute intensity of the Balmer α (6562.8 Å) line measured using the calibrated spectrometer. The spectrometer response was determined to be approximately flat in the 4000-7000 Å region by ion etching and with a tungsten intensity calibrated lamp. The absolute intensities of $n = 4$ to 9 were determined from the absolute intensity of Balmer α ($n = 3$) and the relative intensity ratios.

The VUV spectrometer was a normal incidence 0.2 meter monochromator equipped with a 1200 lines/mm holographic grating with a platinum coating that covered the region 20 – 5600 Å. The VUV spectrum was recorded with a CEM. The wavelength resolution was about 0.2 Å (FWHM) with slit widths of 50 μm. The increment was 2 Å and the dwell time was 500 ms. The VUV spectra (900 – 1300 Å) of the water and control hydrogen plasmas were recorded at 90 W input power.

The spectrometer was calibrated between 400-2000 Å with a standard discharge light source using He, Ne, Ar, Kr, and Xe lines: He I (584 Å), He II (304 Å), Ne I (735 Å), Ne II (460.7 Å), Ar I (1048 Å), Ar II (932 Å), Kr II (964 Å), Xe I (1295.6 Å), Xe II (1041.3 Å), Xe II (1100.43 Å). The wavelength and intensity ratios matched those given by NIST.[21] The spectrometer response was determined to be approximately flat in the 1000-1300 Å region. The calculation of the number density of the $n = 3$ to 9 states was corrected for the minor variation of the sensitivity with wavelength in this region.

The electron density and temperature of the rt-plasma was determined using a compensated Langmuir probe according to the method given previously.[22]

III. Results and Discussion

The high resolution visible spectra (4000-6700 Å) of the cell emission from a hydrogen microwave plasma at 90 W input power (top), a water microwave plasma with 90 W input power (middle), and a water microwave plasma with 50 W input power (bottom) are shown in Figure 1. As shown by the absolute intensity measurements of the Balmer lines of the hydrogen microwave plasma, we observed the known ratios of the Balmer lines. In contrast, the population of the level $n = 4$, $n = 5$, and $n = 6$ of hydrogen was continuously inverted with respect to $n = 3$ in the water plasma. The relative intensities of the Balmer lines of

microwave plasmas of hydrogen (90-2%) mixed with xenon, krypton, or nitrogen at 50 W were equivalent those of hydrogen alone; thus, the inversion is not inherent to a hydrogen plasma generated by microwaves. As shown in Figure 1, when the input power was increased to 90 W, the $n = 5$ and $n = 6$ levels were further continuously inverted with respect to $n = 4$. Thus, wavelength tunebility may be achieved by varying the microwave power with lasing between the corresponding power-dependent inverted levels.

No inversion was observed with RF driven water plasmas as shown in Figure 2. We had shown previously that the conditions of the particular discharge may be a major parameter in the observation of excessive Doppler Balmer line broadening with plasmas of hydrogen and a noble ion having an ionization potential of an integer multiple of E_h.[8-10,15-17] We proposed that the corresponding energetic hydrogen formed with an Evenson microwave cavity may be a means to achieve population inversion.

Other explanations of the overpopulation were ruled out. The spectrometer response was determined to be approximately flat in the 4000-7000 Å region by ion etching and with an intensity calibrated lamp. Furthermore, the Balmer and Lyman line intensity ratios of the control hydrogen plasmas closely matched those obtained using the NIST Einstein A coefficients.[21] Since these ratios did not change as the pressure was lowered, and the hydrogen pressure was lower in the water plasma than the control, the NIST Einstein A coefficients were used to calculate the number density ratios from the water plasma emission.

The water plasma was determined to be optically thin for water absorption of hydrogen Balmer and Lyman lines; thus, absorption of 6562.8 Å and 4861.3 Å and 1215.67 Å emission by $n = 2$ and $n = 1$ state atomic hydrogen, respectively, may be neglected as the cause of the inverted ratios. The absorption cross section of Balmer emission by water is insignificant.[23] Thus, the Balmer lines were used to determine the lasing conditions except for the $n = 2$ level

which was determined from the intensities of the Lyman lines. Using the absorption cross section of water for Lyman α emission of $\sigma = 1.6 \, X \, 10^{-17} \, cm^2$,[24] the water plasma was determined to be optically thin by the method given previously[25] since the water number density, $N_{H_2O} = 2.5 \, X \, 10^{15} \, cm^{-3}$, was low, and the path length, 5 cm, was short.

To further characterize the water plasma, the width of the 6562.8 Å Balmer α line ($n = 3$ to $n = 2$) was measured on light emitted from the microwave discharges of water vapor and pure hydrogen alone using the high resolution visible spectrometer. The method of Videnovic et al.[26] was used to calculate the hydrogen atom energies and densities from the line width. Significant line broadening of 55 eV and an atom density of $6 \, X \, 10^{13} \, atoms/cm^3$ was observed from the water plasma compared to an average hydrogen atom temperature of 1 eV and a density of $6 \, X \, 10^{11} \, atoms/cm^3$ for hydrogen alone. We have assumed that Doppler broadening due to thermal motion was the dominant source in the water plasmas to the extent that other sources may be neglected. In general, the experimental profile is a convolution of two Doppler profiles, an instrumental profile, the natural (lifetime) profile, Stark profiles, van der Waal's profiles, a resonance profile, and fine structure. The source of broadening was confirmed to be Doppler alone by considering each possible source according to the methods described previously.[15-18] Similarly, using a compensated Langmuir probe as described previously,[22] the electron temperature, T_e, measured on the microwave water plasmas was higher, 2.0 eV, compared to the $T_e < 1 \, eV$ measured on the hydrogen plasma at the same 50 W input power.

No hydrogen species, H^+, H_2^+, H_3^+, H^-, H, or H_2, of the water plasmas responds to the microwave field; rather, only the electrons respond. However, the measured electron temperature in these microwave plasmas was about 1-2 eV; whereas, the measured neutral

hydrogen temperature was much higher, 55 eV. This requires that $T_i \gg T_e$ which can not be due to direct ion coupling to the microwave power or electron-collisional excitation. Nor, can this result be explained by electric field acceleration of charged species as proposed for glow discharges[26-28] since in microwave driven plasmas, there is no high electric field in a cathode fall region ($> 1 \; kV/cm$) to accelerate positive ions. The observation of excessive Balmer line broadening in a microwave driven plasma requires a source of energy. In the case of the water plasma, we propose that the source is the energy is due to a resonant energy transfer between hydrogen atoms and oxygen. The catalysis mechanism was supported by the observation of O^{2+} at 2454.9 and 2558.0 Å as well as the extraordinary line broadening Balmer line broadening of 55 eV compared to 2 eV for hydrogen alone. This energy may be the basis of the pumping source for the observed population inversions.

Then the inverted population is explained by a resonance energy transfer between hydrogen and oxygen to yield fast $H(n = 1)$ atoms. The emission of excited state H from fast $H(n = 1)$ atoms excited by collisions with the background H_2 has been discussed by Radovanov et al.[28] Formation of H^* is also predicted by a collisional radiative model,[25] which is far from thermal equilibrium in terms of the hydrogen atom temperature. Akatsuka et al.[6] show that it is characteristic of cold recombining plasmas to have the high lying levels in local thermodynamic equilibrium (LTE); whereas, for the low lying levels, population inversion is obtained when T_e becomes low with an appropriate electron density as shown by the Saha-Boltzmann equation.

The absolute reduced Balmer population density of the excited hydrogen atoms $\dfrac{N_n}{g_n}$ with principal quantum numbers $n = 1$ to 9 were obtained from N, their absolute intensity integrated over the visible spectral peaks corrected by their Einstein coefficients, divided by g,

the statistical weight ($g = 2n^2$), as discussed by Akatsuka et al.[6] As given in Table 1, $\dfrac{N_n}{g_n}$ for

quantum number $n = 3,4,5,6$ recorded on a water microwave plasma at 90 W input was

determined to be $3.44 \, X \, 10^8 cm^{-3}$, $3.44 \, X \, 10^8 cm^{-3}$, $9.02 \, X \, 10^8 cm^{-3}$, and $385 \, X \, 10^8 cm^{-3}$,

respectively.

To determine the population of the $n = 2$ level, VUV spectra (900 – 1300 Å) were

recorded on light emitted from water and hydrogen microwave discharge plasmas at 90 W

input power. As shown in Figure 3, the Lyman series was also inverted. From the number

densities of the levels determined from the absolute Balmer line intensities given in Table 1

and the Lyman lines intensities shown in Figure 3, it was found that

$$\frac{N_4}{N_3} \text{Balmer} = 4.66; \quad \frac{N_4}{N_3} \text{Lyman} = 4.46$$

Since $\dfrac{N_4}{N_3}$ determined from the Lyman series and the Balmer series was about the same, and the

Balmer α line was absolutely measured, the absolute number density for $n = 2$ given in Table

1 was determined from the absolute Balmer α line intensity.

$$(N_2)_{\text{Balmer}} = (N_3)_{\text{Balmer}} \times \left(\frac{(N_2) Lyman}{(N_3) Lyman} \right)$$

Using $N_3 = 6.20 \, X \, 10^9 \, cm^{-3}$ and $g_2 = 8$, $\dfrac{N_2}{g_2}$ was determined to be $1.74 \, X \, 10^8 \, cm^{-3}$.

With appropriate cavity length and mirror reflection coefficient, cw laser oscillations

may be obtained between states having an overpopulation ratio determined by $\dfrac{N_i}{N_f} \dfrac{g_f}{g_i} > 1$ as

shown in Table 1 where i represents the quantum number of the initial state and f represents

that of the final state.[6] On this basis, it was determined that lasing is possible over a wide range

10

from far infrared to violet wavelengths. Representative transitions and wavelengths are shown in Table 2. The important parameter for lasing is that the reduced overpopulation density is above threshold. Using standard laser cavity equations,[6] it was determined that the threshold condition is achievable with micron to submillimeter laser cavities for several transitions emitted from these plasmas. For plasma properties of this experiment determined using a Langmuir probe ($T_e = 2.0$ eV, electron density $n_e = 0.2 \times 10^8$ cm^{-3}), conditions for lasing at 12,818.1 Å, 4340.5 Å, and 4101.7 Å corresponding to the transitions $5 \rightarrow 3$, $5 \rightarrow 2$, and $6 \rightarrow 2$, respectively, were determined assuming a cavity length of 100 cm and a combined mirror reflection coefficient of 0.99, as given in Table 3. The overpopulation ratios $\dfrac{N_5}{N_3}\dfrac{g_3}{g_5}$, $\dfrac{N_5}{N_2}\dfrac{g_2}{g_5}$, and $\dfrac{N_6}{N_2}\dfrac{g_2}{g_6}$ given in Table 1 were 112, 221, and 67, respectively. Threshold reduced $n = 5$ overpopulation densities of about 0.49×10^7 cm^{-3} and 4.6×10^7 cm^{-3} are required for lasing to $n = 3$ and $n = 2$, respectively, and, a corresponding threshold reduced $n = 6$ overpopulation density of 6.9×10^7 cm^{-3} is required for lasing to $n = 2$. The actual reduced overpopulation densities were much greater, 3.8×10^{10} cm^{-3}, 3.8×10^{10} cm^{-3}, and 1.2×10^{10} cm^{-3}, respectively. Thus, lasing is expected with cavity lengths of 0.01 cm, 0.2 cm, and 0.6 cm, respectively.

Lasing is possible at blue wavelengths which are ideal for many communications and microelectronics applications as well as at a wavelength of 1.3 μm which is ideal for transmission through glass optical fibers. The emission wavelength of the potential water laser is about 400 nm which is suitable for the next generation 15-Gbyte DVDs.[1] Currently, the ideal laser diode for telecommunications applications is the $In_x Ga_{1-x} As_y P_{1-y}$ diode laser wherein a lattice constant mismatch requires that the laser be separate from the silicon circuits.

An integrated laser would revolutionize telecommunications, electronics, and computing.[29] Conceptually, we see no obvious impediment to integration of a water-plasma laser. In addition, many more laser wavelengths corresponding to Balmer, Paschen, and Brackett lines are possible. With the capability of lasing over the widest range of atomic wavelengths of any known atomic laser, far infrared to violet, the hydrogen laser based on water-plasma may prove to be the most versatile laser yet discovered.

References

(1) Nakamura, S. *Science* **281**, 956 (1998).

(2) Hardin, R. W. "Challenges remain for blue diode lasers" (OE Reports, SPIE 192, December 1999; http://www.spie.org/web/oer/december/dec99/cover1.html).

(3) Gudzenko, L. I.; Shelepin, L. A. *Sov. Phys. JEPT* **1963**, *18*, 998.

(4) Suckewer, S.; Fishman, H. *J. Appl. Phys.* **1980**, *51*, 1922.

(5) Silfvast, W. T.; Wood, O. R. *J. Opt. Soc. Am. B* **1987**, *4*, 609.

(6) Akatsuka, H.; Suzuki, M. *Phys. Rev. E* **1994**, *49*, 1534–1544.

(7) Mills, R.; Dong, J.; Lu, Y. *Int. J. Hydrogen Energy* **2000**, *25*, 919–943.

(8) Mills, R.; Nansteel, M.; Ray, P. *IEEE Trans. Plasma Sci.* **2002**, *30* (2), in press.

(9) Mills, R. L.; Ray, P.; Dhandapani, B.; Nansteel, M.; Chen, X.; He, J. *J. Quant. Spectros. Radiat. Transfer*, **2002**, in press.

(10) Mills, R.; Ray, P. *J. Mol. Struc.* , **2002**, in press.

(11) Linde, D. R. *CRC Handbook of Chemistry and Physics*, 79th ed; CRC Press: Boca Raton, Florida, **1998-9**; pp 10-175–10-177.

(12) Crocker, A.; Gebbie, H. A.; Kimmitt, M. F.; Mathias, L. E. S. *Nature* **1964**, *201*, 25.

(13) Sarjeant, W. J.; Kucerovsky, Z.; Brannen, E. *Appl. Opt.* **1972**, *11*, 735.

(14) Shuaibov, A. K.; Dashchenko, A. I.; Shevera, I. V. *Quant. Electron.* **2001**, *31*, 547.

(15) Mills, R. L.; Ray, P.; Dayalan, E.; Dhandapani, B.; He, J. *IEEE Trans. Plasma Sci.*, (To be published).

(16) Mills, R.; Ray, P. *New J. Phys.* **2002**, *4*, 22.1–22.17.

(17) Mills, R.; Ray, P.; Dhandapani, B.; He, J. *J. App. Phys.*, (To be published, MS#JR02-0987).

(18) Fehsenfeld, F. C.; Evenson, K. M.; Broida, H. P. *Rev. Sci. Instrum.* **1965**, *35*, 294.

(19) McCarroll, B. *Rev. Sci. Instrum.* **1970**, *41*, 279.

(20) Tadic, J.; Juranic, I.; Moortgat, G. K. *J. Photochem. Photobiol, A*, **2000**, *143*, 169–179.

(21) NIST Atomic Spectra Database, www.physics.nist.gov/cgi-bin/AtData/display.ksh.

(22) Barton, D.; Bradley, J. W.; Steele, D. A; Short, R. D. J. *Phys. Chem. B* **1999**, *103*, 4423–4430.

(23) Calvert, J. G.; Pitts, J. N. *Photochemistry*, John Wiley and Sons: New York, **1966**, pp. 200–202.

(24) Vatsa, R. K.; Volpp, H. R.; *Chem. Phys. Lett.* **2001**, *340*, 289.

(25) Mills, R.; Ray, P.; Mayo, R. *J. Vac. Sci. Technol. A*, submitted.

(26) Videnovic, I. R.; Konjevic, N.; Kuraica, M. M. *Spectrochim. Acta, Part B* **1996**, *51*, 1707–1731.

(27) Kuraica, M.; Konjevic, N. *Phys. Rev. A* **1992**, *46*, 4429–4432.

(28) Radovanov, S. B.; Dzierzega, K.; Roberts, J. R.; Olthoff, J. K. *Appl. Phys. Lett.* **1995**, *66*, 2637–2639.

(29) Ball, P. *Nature* **2001**, *409*, 974–976.

Table 1. Level densities N_n, reduced population densities $\dfrac{N_n}{g_n}$ [a], and overpopulation

ratios $\dfrac{N_n}{N_2}\dfrac{g_2}{g_n}$, $\dfrac{N_n}{N_3}\dfrac{g_3}{g_n}$, and $\dfrac{N_n}{N_4}\dfrac{g_4}{g_n}$ for excited states $n = 1$ to 9 with an $n > 2$ pumping

mechanism recorded on a water microwave plasma at 90 W input power.

principal quantum number n	$N_n (10^9\ cm^{-3})$	$\dfrac{N_n}{g_n} (10^8\ cm^{-3})$	$\dfrac{N_n}{N_2}\dfrac{g_2}{g_n}$	$\dfrac{N_n}{N_3}\dfrac{g_3}{g_n}$	$\dfrac{N_n}{N_4}\dfrac{g_4}{g_n}$
1	60,000 [b]	30,000	—	—	—
2	1.39	1.74	—	—	—
3	6.20	3.44	1.98	—	—
4	28.9	9.02	5.18	2.62	—
5	1930	385	221	112	42.7
6	838	116	66.7	33.7	12.9
7	47.4	4.83	2.78	1.40	0.535
8	26.1	2.04	1.17	0.593	0.226
9	15.3	0.955	0.549	0.278	0.106

[a] $g_n = 2n^2$ and n is the principal quantum number

[b] calculated after ref. (26)

Table 2.   Potential laser transitions of atomic hydrogen in a microwave water-vapor plasma.

wavelength/Å	spectral region	electronic transition $n_{initial} - n_{final}$
74,578	IR	$6 \rightarrow 5$
40,512	IR	$5 \rightarrow 4$
26,252	IR	$6 \rightarrow 4$
18,751	IR	$4 \rightarrow 3$
12,818	IR	$5 \rightarrow 3$
10,938	IR	$6 \rightarrow 3$
10,049	IR	$7 \rightarrow 3$
6,563	red	$3 \rightarrow 2$
4,861	blue	$4 \rightarrow 2$
4,340	violet	$5 \rightarrow 2$
4,102	violet	$6 \rightarrow 2$
3,970	violet	$7 \rightarrow 2$
3,889	violet	$8 \rightarrow 2$

Table 3. Observed reduced overpopulation densities recorded on a water microwave plasma at 90 W input power, threshold overpopulation densities for lasing with a 100 cm length cavity, and the minimum laser cavity length to achieve lasing for the observed reduced overpopulation densities for the transitions, 5-2, 5-3, and 6-2.

laser transition	ΔE (eV)	wavelength (Å)	A_{ki} [a] $10^8 s^{-1}$	reduced overpopulation density (10^{10} cm^{-3})	threshold reduced overpopulation density [b] (10^7 cm^{-3})	minimum length (cm)
5-2	2.86	4340.5	0.0943	3.83	4.61	0.212
5-3	0.966	12,818.1	0.0339	3.82	0.494	0.013
6-2	3.02	4101.7	0.0515	1.15	6.92	0.605

[a] Einstein A coefficient for the transition from level k to level i

[b] for a laser cavity length of 100 cm

Figure Captions

Figure 1. The visible spectra (4000-6700 Å) of the cell emission from a hydrogen microwave plasma at 90 W input power (top), a water microwave plasma with 90 W input power (middle), and a water microwave plasma with 50 W input power (bottom). Stationary inverted H Balmer populations were observed from the low pressure water-vapor microwave discharge plasmas. The population of the level $n = 4, 5$, and 6 of hydrogen was continuously inverted with respect to $n = 3$ at 50 W and at 90 W input power to the water plasma; whereas, when the input power was increased to 90 W, the $n = 5$ and 6 levels were further continuously inverted with respect to $n = 4$.

Figure 2. The visible spectra (4000-7200 Å) of the cell emission from water microwave (top) and inductively coupled RF (bottom) plasmas with 90 W input power. The population of the levels $n = 4, 5, 6, 7, 8$, and 9 of hydrogen was continuously inverted with respect to $n = 2$ and $n = 3$ in the water microwave plasma; whereas, no inversion was observed in the RF plasma.

Figure 3. The VUV spectra (900 – 1300 Å) of the cell emission from hydrogen microwave and the water microwave plasmas with 90 W input power. An inverted Lyman population was observed from the water plasma emission with the inversion observed in the visible as shown in Figure 1 extending to the $n = 2$ level.
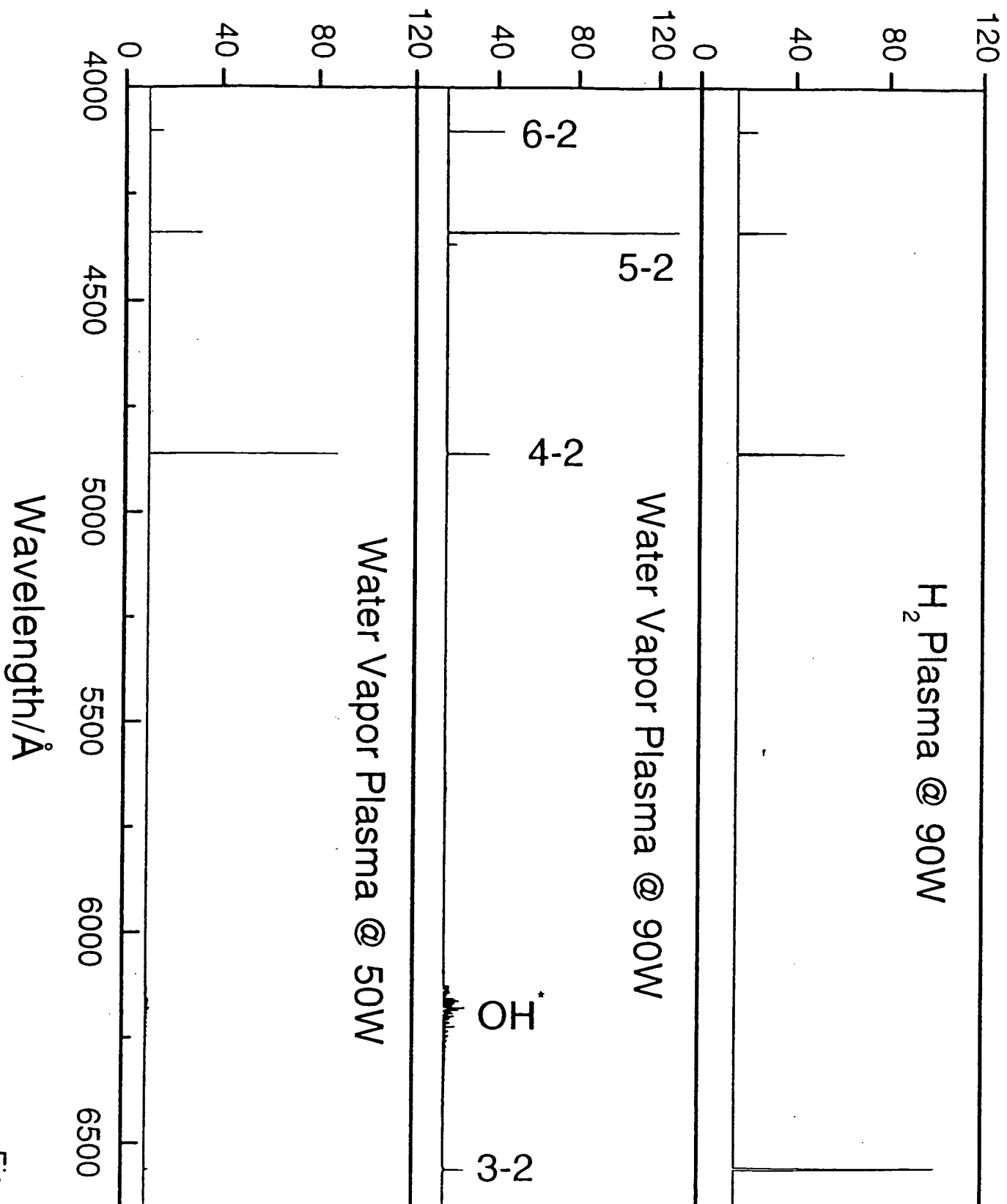
Fig. 1

Intensity/Arb. Unit

Wavelength/Å

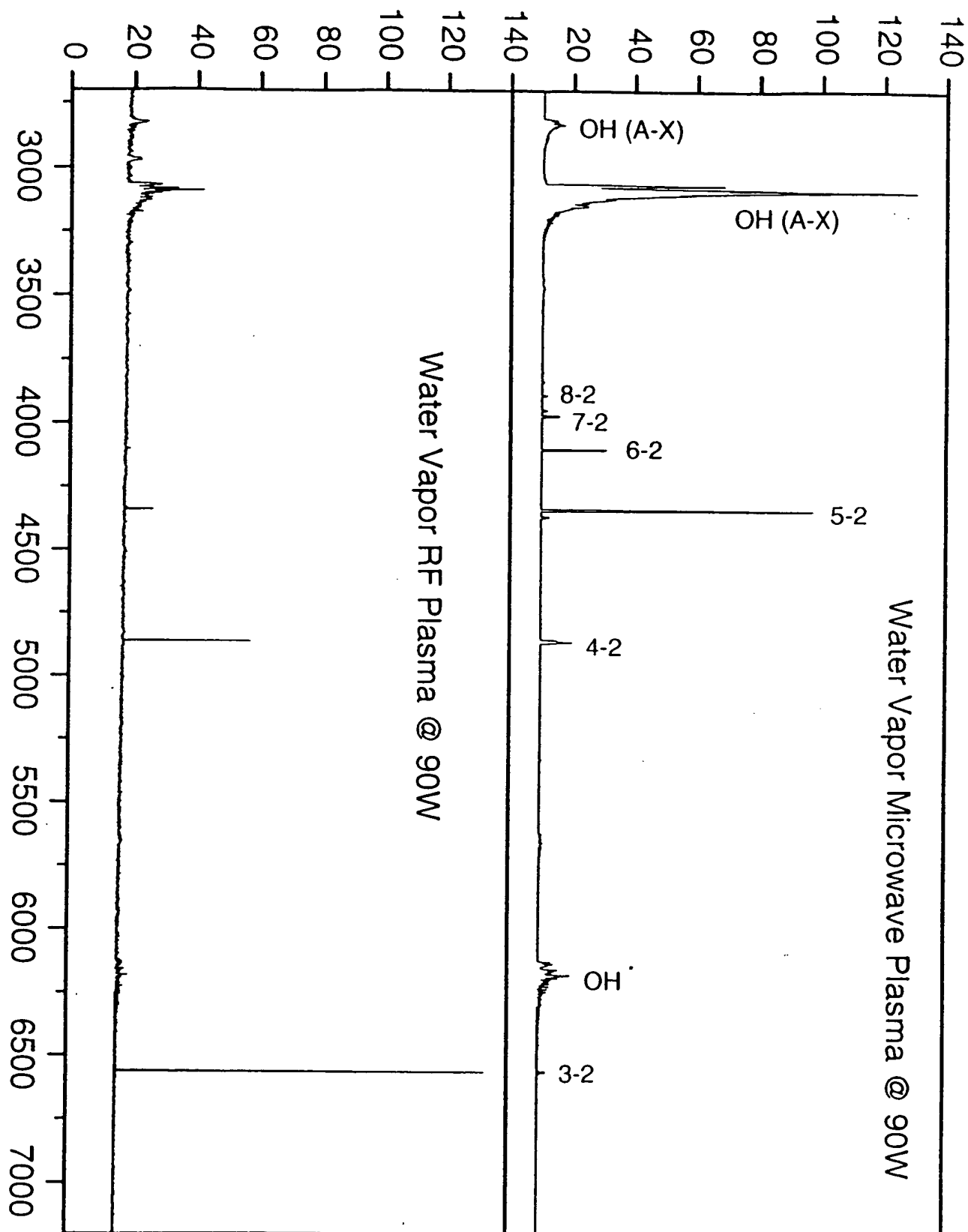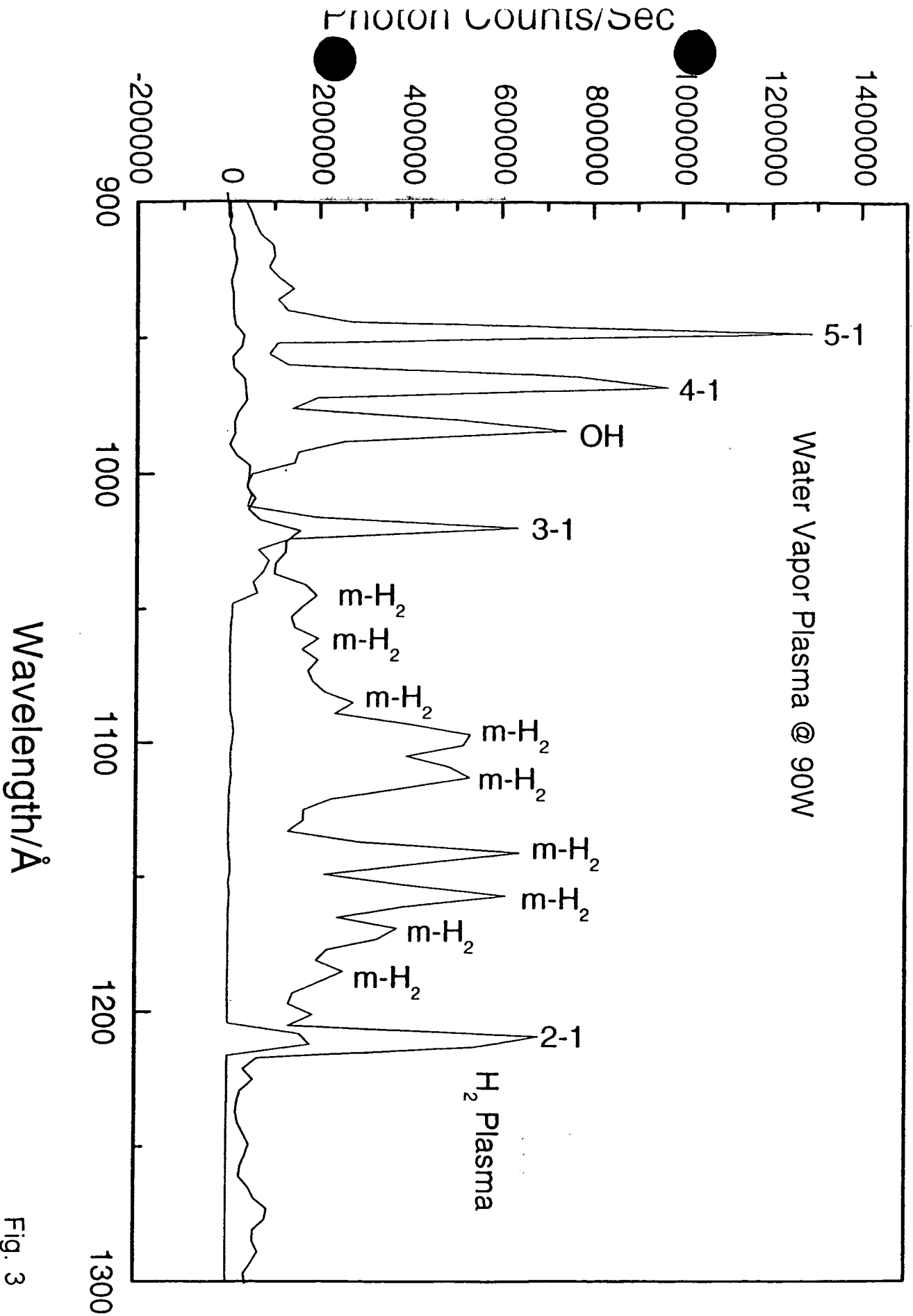H₂ Plasma @ 90W

Water Vapor Plasma @ 90W

Water Vapor Plasma @ 50W

6-2

5-2

4-2

3-2

OH*

Fig. 2

Fig. 3